Volume 9 Number 13 1981 Nucleic Acids Research

Circular dichroism spectra of twelve short DNA restriction fragments of known sequence: a comparison of measured and calculated spectra

Wolfgang Hillen*, Thomas C.Goodman and Robert D.Wells

University of Wisconsin, Department of Biochemistry, College of Agricultural and Life Sciences, Madison, WI 53706, USA

Received 6 May 1981

ABSTRACT

The CD spectra of twelve DNA restriction fragments ranging in size from 12 to 360 base pairs are reported. Since the sequences of these fragments are known, it is possible to calculate their CD spectra from a set of nearest neighbor contributions derived from a combination of synthetic polydeoxyribonucleotides. While the calculations lead to good agreement in the negative band at approximately 245 nm, they generally reproduce the positive band at approximately 270 nm only poorly. The experimentally observed positive band consists of two peaks centered around 270 and 285 nm. The comparison of calculated and measured spectra reveals that end effects lead to increased disagreement for fragments smaller than approximately 40 base pairs. The disagreement between calculated and measured spectra can be partially attributed to the fraction of next nearest neighbors in the DNAs, which are also in the spectral components. Thus, the sequence specific CD contributions in the long wavelength region of the spectra extend at least to next nearest neighbor nucleotides and may extend beyond.

INTRODUCTION

Circular dichroism (CD) spectroscopy has been used in a wide variety of studies to obtain structural information about nucleic acids (1-6). The CD spectrum of a given DNA depends on both its secondary structure (4,7) and nucleotide sequences (1,8). Samples examined by CD include synthetic polynucleotides (5,7-10), chromosomal DNAs (11,12), satellite DNAs (9,13), and restriction fragments (6,14). In general, while the negative CD band with a maximum amplitude at approximately 245 nm appears to be relatively independent of the AT content and secondary structure of the DNA (11,12), the positive band with a maximum amplitude at approximately 275 nm is sensitive to the base composition and the secondary structure of the molecule (4,11, 12).

Some evidence suggests that the CD spectrum of a given DNA may depend in large part on the CD contributions of the nearest neighbor base pairs in its polynucleotide chain (15). Using this nearest neighbor approximation,

Gray and Tinoco (16) showed that a "basis set" of eight CD spectra of DNAs with known and linearly independent nearest neighbor frequencies is sufficient to allow either the calculation of the CD spectrum of another DNA (based on its known nearest neighbor frequencies) or, in reverse, the calculation of the DNAs nearest neighbor frequencies based on its known CD spectrum.

In an early study employing this technique, Allen et al. analyzed different satellite DNAs using a basis set derived from chromosomal DNAs and synthetic polymers (9). While there were difficulties in the interpretation for these AT-rich DNAs, an improved basis set of spectra were able to partially overcome these problems (13,15).

With additional CD spectra of repeating DNA polymers, it is possible to construct over 90 different basis sets. Each of these sets yields a matrix of spectral components (T-matrix) from which CD spectra can be calculated. Gray et al. evaluated the ability of 21 of these matrices to predict nearest neighbor frequencies from the CD spectra of "unknown" DNAs (15). The best results overall were obtained with T-matrix 14.

The combined use of gene cloning and high pressure liquid chromatography on RPC-5 (reviewed in 2) has made available large quantities of homogeneous DNA restriction fragments. Since these fragments (2,17-19) have known nucleotide sequences, it is possible to evaluate the ability of the T-matrices to predict the observed CD spectra. Hence, the validity of the nearest neighbor CD approximation can be tested for homogeneous samples that are small enough to exclude averaging of possible sequence specific contributions. In this study, the experimentally determined spectra for fragments varying in size from 12- to 360-bp are compared with CD curves calculated from spectral components derived from sets of synthetic DNA polymers (T-matrices 1 and 14).

MATERIALS AND METHODS

DNA samples

The DNA fragments were prepared from pRW574 essentially as described (17). The fragments were free of contaminating DNA fragments (>98% pure) after final RPC-5 fractionation as demonstrated by polyacrylamide gel electrophoresis. In addition, the general absence of contaminants in these and related fragments purified by this method has been demonstrated by other techniques including in vitro DNA replication (20), in vitro transcription (21-25), CD (6,14), proton and ^{31}P-NMR (6,26-28), reactions

with other restriction enzymes or DNA ligase (19,29), high resolution helix-coil transitions (25,30-32), DNA sequence studies (33), and laser Raman spectroscopy (34). Prior to the CD measurements, all fragments were dialyzed exhaustively against 10 mM Na cacodylate (pH 7.0), 0.1 mM EDTA. The concentration of the samples varied between 0.3 and 0.5 A_{260}/ml.

Optical measurements

A recording Jasco model J-41 C spectropolarimeter was used for the CD measurements. Prior to each series of determinations the ellipticity scale was calibrated to 0.3133° at 290 nm using a 0.1% solution of d10-camphor sulfonic acid. The ellipticity of the samples was measured at ambient temperature (22-25°C) using quartz cuvettes with a one cm optical pathlength. After the CD spectra were obtained, the absorption of the samples was measured using a Cary 219. The CD spectra were digitized at 2.5 nm intervals from 307.5 to 210.0 nm, and the data were converted to $\Delta\varepsilon$/mole of monomer using the extinction coefficients from ref. 11 and the known GC content of the DNA fragments. The CD spectra were reproducible to within $\pm$2%.

Calculation of the CD spectra and next nearest neighbor frequencies

T-matrices 1 and 14 were generated as previously described (9,16) from the CD spectra of repeating DNA polymers (15,35). CD spectra for each of the fragments were calculated from these matrices using the known nearest neighbor frequencies of the DNAs (9, and the refs. in Table 1). Single stranded ends, created as a result of restriction enzyme digestion, are not included in the sizes reported for these fragments, nor were they considered in the calculation of the predicted spectra.

The polymers employed in T-matrix 14 contain 32 of the 64 possible next nearest neighbor combinations. The sequences ApTpA, TpApT, GpApG, and CpTpC are each represented twice giving 36 total next nearest neighbors. In the same way, the polymer sequences present in the basis set of T-matrix 1 contain only 28 next nearest neighbor combinations. In order to equalize the number of next nearest neighbors present in each T-matrix, the sequences unique to T-matrix 1, namely ApApA, TpTpT, GpGpG, and CpCpC were scored as three rather than one when they were encountered in the DNA sequences, the fraction of next nearest neighbors included in a given T-matrix was computed by determining the number of next nearest neighbor sequences present in both the DNA and also represented in the polymer basis set and dividing this number by the total number of next nearest neighbors in the DNA. A PDP 11/03 computer (Digital Equipment Corp.) was used for the sequence

analysis of the DNAs and all other calculations. Both experimental and calculated spectra were plotted with a Hewlett-Packard model 7245A plotter-printer.

RESULTS

Characteristics of DNAs

The sequenced DNA restriction fragments used in this study originate from the E. coli lactose control region and from the plasmid pVH51 (36). Table 1 summarizes some of their sequence characteristics. It is important in this study that the DNAs are homogeneous in size and contain no contaminating fragments. Thus, gel analysis of the fragments was done immediately prior to the CD measurements and then repeated after the final absorption measurements were taken. The result from this final analysis was identical to the first determination and is shown in Fig. 1.

Several of these fragments are of special interest since they contain known protein binding sites. Both E. coli RNA polymerase and lac repressor proteins bind to specific regions in the 95-bp fragment. The 360-bp fragment contains at least two promoters (24), and the 43-bp fragment is part of the origin of replication (40) of pVH51.

Salt and counterion effects on the observed CD spectra

The basis set CD spectra used to generate the T-matrices were measured (15) under counterion conditions slightly different from those used in the present study. To determine if small changes in the Na^+ concentration or the substitution of cacodylate for phosphate would affect the measured CD curves, the 22-, 43-, and 258-bp fragments were dialyzed into 10 mM sodium phosphate buffer (pH 7.0) containing 0.1 mM EDTA and their CD spectra were redetermined. No significant changes (average $\sigma<0.10$) were observed.

Comparison of observed and calculated CD spectra

Two different matrices, T-matrix 1 and T-matrix 14, were used in generating the calculated CD spectra. The calculated spectra generated with T-matrix 14 are much closer in their agreement with the experimentally measured spectra than those produced with T-matrix 1. Hence, a detailed comparison of the T-matrix 14 calculated curves and the experimentally measured spectra is presented first, followed by a comparison with the T-matrix 1 curves.

Fig. 2 shows the experimentally measured CD spectra of the 12-, 17-, 22-, and 27-bp fragments as well as the calculated spectra and the average of the two calculated spectra. The agreement between the calculated and

TABLE 1. Sequence characteristics of the DNA fragments.

No. of base pairs in the fragment[a]	Source	% GC	% purines in + strand	Fract. NNNs in T-matrix[b] 1	14	% [AA+TT+ GG+CC]	Ref. for sequence
12	pVH51	66.7	50.0	0.70	0.70	16.6	37, 38
17	lac	41.2	41.2	0.33	0.73	29.4	39
22	lac	63.6[a]	68.2[a]	0.55[a]	0.55[a]	31.8	39
27	lac	44.4[a]	48.2[a]	0.44[a]	0.64[a]	18.5	39
43	pVH51	48.8	20.9	0.59	0.54	34.5	40
64	lac	54.7	59.4	0.58	0.56	24.5	39
69	pVH51	52.2	42.0	0.60	0.66	21.7	37, 38
76	lac	61.8	44.7	0.80	0.42	31.6	39
84	pVH51	59.5	57.1	0.50	0.48	30.9	37, 38
95	lac	46.3	47.4	0.65	0.70	26.8	39
258	pVH51	54.7	52.7	0.66	0.52	30.0	37, 38
360	pVH51	29.4[a]	50.8[a]	0.73[a]	0.73[a]	30.3	40, 24

a) Single-stranded Eco RI ends, present in the 22-, 27-, and 360-bp fragments, are not considered in calculating these values.

b) The fraction of next nearest neighbors (NNNs) present for each T-matrix = Σ(NNNs in both the sequence and T-matrix)/total number of NNNs present in the sequence.

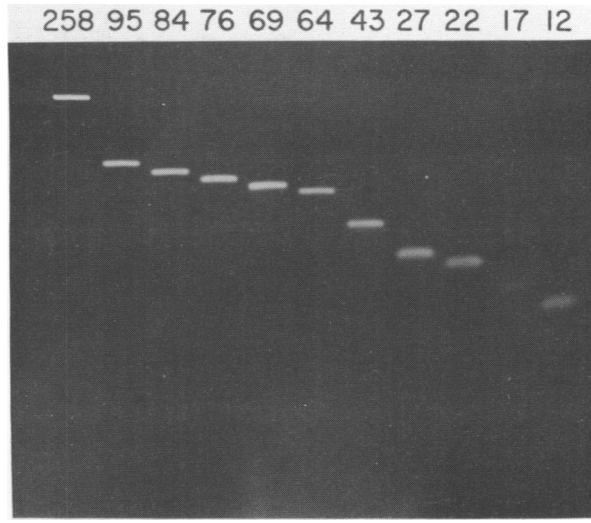

Figure 1. Polyacrylamide gel analysis of the fragments. 0.2-0.5 µg of each DNA fragment was electrophoresed on an 8% polyacrylamide, 10% glycerol gel. The numbers at the top refer to the size of each fragment (in bp) excluding single-stranded ends.

measured spectra is only very general. Whereas the shape of the spectra is similar, the detailed features differ significantly for these short DNA helices. The amplitudes of the positive and negative bands of the 12-bp fragment in Fig. 2A are about 25% lower than the T-matrix 14 calculation predicts. Also, although the wavelength of maximal and minimal $\Delta\varepsilon$ agree quite well, the calculated spectrum exhibits a large shoulder on the long wavelength side of the positive band at approximately 285 nm which is not found for the observed spectrum. The low wavelength part of this spectrum around 215 nm also disagrees with the spectrum calculated from nearest neighbor contributions. The 17-bp fragment displays similar deviations of the measurement from calculation. The amplitudes of both the negative (245 nm) and positive (270 nm) bands are significantly smaller for the observed spectra. Also, as for the 12-bp fragment, the calculation produces a higher amplitude around 285 nm than is experimentally measured.

While the maximum amplitude for the negative band of the 27-bp fragment is shifted to 247 nm, in general the agreement between measurement and calculation in this region is very good for both the 22- and 27-bp fragments. With regard to the positive band, the measured spectra of these

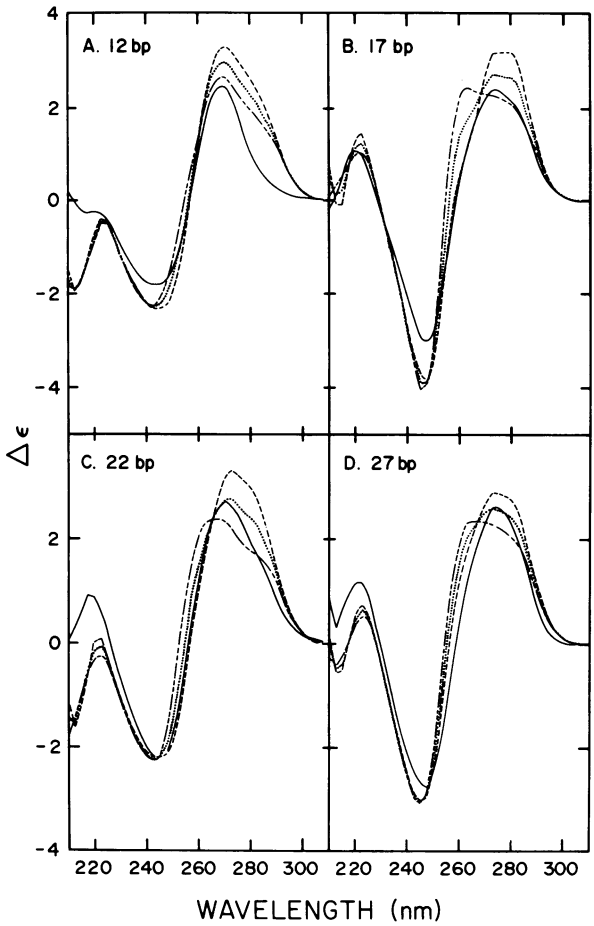

Figure 2. Measured and calculated CD spectra for the 12-, 17-, 22-, and 27-bp fragments. The measured CD spectra are shown as solid lines. The evenly dashed lines (-----) in each panel represent the T-matrix 14 calculated CD spectrum of the respective fragment. The unevenly dashed lines (—— —) give the CD spectra calculated with T-matrix 1, and the dotted lines show the average of the two calculated spectra for each of the fragments.

fragments are narrower than predicted by the calculation. Whereas the 27-bp fragment shows the smallest deviation of the measured from the T-matrix 14 calculated spectrum among the four short fragments (Fig. 2), the positive band of the 22-bp DNA deviates more significantly from this calculation. The positive contribution observed in the calculated spectrum around 285 nm does not appear in the measured spectrum for this fragment. The $\Delta\varepsilon$ around 215 nm differs in both cases from the calculation.

Fig. 3 displays CD data for the 43-, 64-, 69-, and 76-bp fragments. The 43-bp fragment shows only very poor agreement with the calculated spectra in the positive band. The negative band seems to be shifted by 2-3 nm to longer wavelengths in the spectrum calculated using T-matrix 14. This is also observed for the 69- and 76-bp fragments. The same displacement,

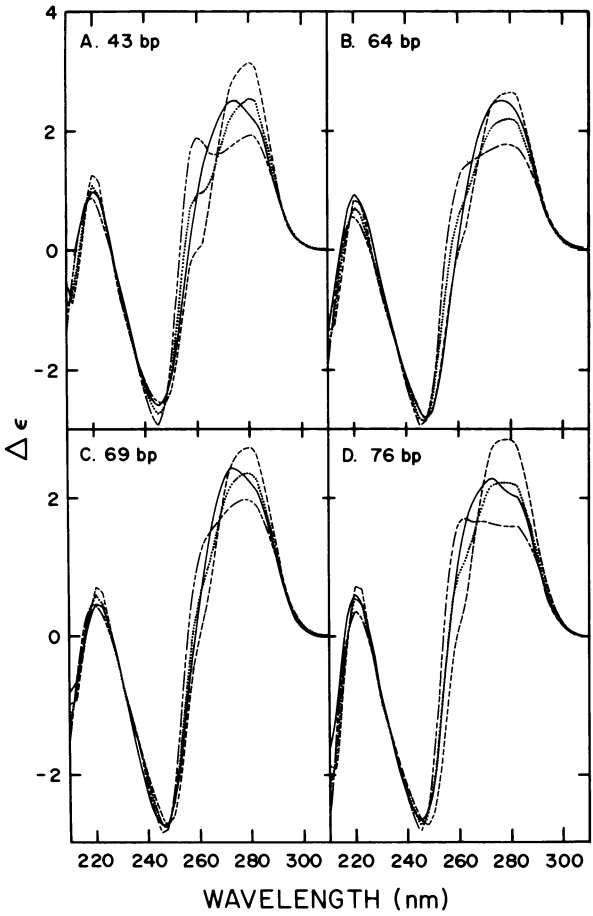

Figure 3. Measured and calculated CD spectra for the 43-, 64-, 69-, and 76-bp fragments. The use of the four different line types in each of the panels is as described in Fig. 2.

though in the opposite direction, was previously noted for the 27-bp fragment. The deviations in the positive bands for all four fragments in Fig. 3 are somewhat similar. The measured bands appear to be shifted to the shorter wavelengths by about 10 nm in the case of the 43-bp fragment and by about 5 nm for the others relative to the T-matrix 14 calculated spectra. With the exception of the 64-bp fragment, the experimentally determined spectra in Fig. 3 suggest that the positive peak is split into two overlapping bands with maxima at approximately 270 and 285 nm. All four fragments show good agreement between measurement and calculation in the short wavelength region of the spectra around 215 nm.

Fig. 4 shows the spectra of the 84-, 95-, 258-, and 360-bp fragments. Except for the 360-bp fragment, the negative bands agree well with the cal-

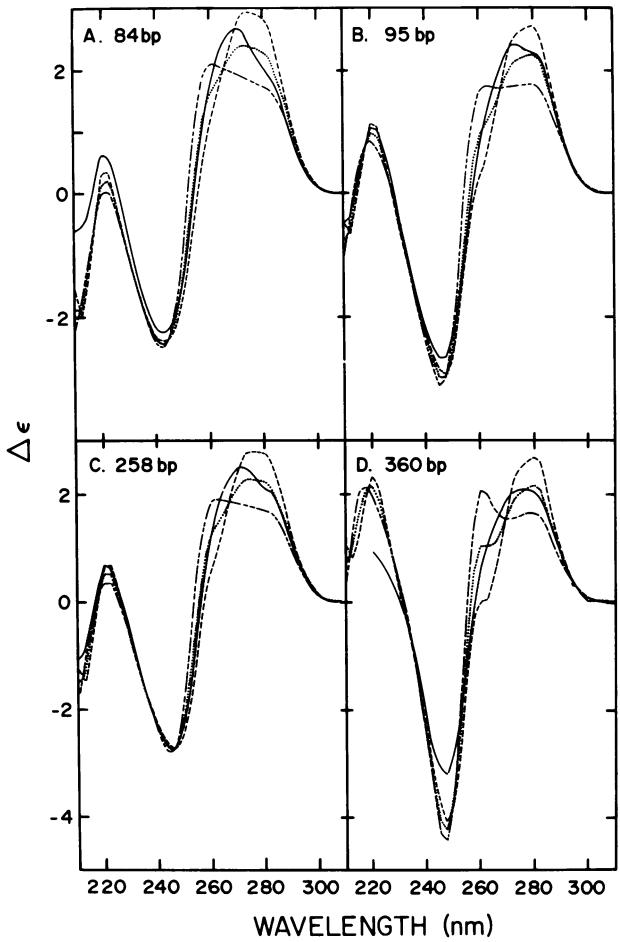

Figure 4. Measured and calculated CD spectra for the 84-, 95-, 258-, and 360-bp fragments. The use of the four different line types in each of the panels is as described in Fig. 2.

culated bands. Only the 258-bp DNA shows the familiar 2-3 nm negative band displacement relative to the T-matrix 14 calculated curve. In addition, the negative band in the 360-bp spectrum reaches only about 75% of the amplitude suggested by the nearest neighbor calculation. The differences between the observed and calculated CD spectra for the 84-, 95-, and 258-bp DNAs are similar to those found for the other fragments in Fig. 3. The positive bands in these three spectra again seem to consist of two overlapping bands with maxima at approximately 270 and 285 nm. The agreement between experiment and calculation is very poor for the 360-bp fragment and fair for the 95-bp fragment. The 84- and 258-bp fragments show larger deviations in their positive bands. All four show satisfactory agreement at short wave-

lengths around 215 nm.

When the spectra calculated using T-matrix 1 are compared to the measured spectra, the following general differences are observed (Figs. 2-4): a) The positive bands in the measured curves have larger amplitudes than the calculated bands; moreover, the calculated band is displaced toward shorter wavelengths relative to the experimental curve. b) The positive bands in the calculated curves are broader than the experimental curves and seem to be composed of two different peaks. c) The negative bands in the calculated spectra generally have a larger amplitude than found for the observed curves and, especially in the case of the smaller fragments (Fig. 2), their minima is displaced toward the shorter wavelengths compared to the measured spectra.

Calculation of standard deviations and normalization of measured spectra

In comparing the observed and calculated CD curves for these fragments, the standard deviation was determined at 2.5 nm intervals from 230.0 to 307.5 nm according to the equation:

$$\sigma = [\Sigma(\text{calculated} - \text{measured})^2/31]^{1/2}$$

The standard deviations obtained between the calculated curves produced with the two T-matrices and the experimentally measured spectra are listed in Table 2.

To eliminate any differences among the measured spectra that could result from errors in approximating the extinction coefficients, the measured spectra were normalized by multiplying each amplitude by the ratio of $\Delta\varepsilon_{\text{measured}}$ at 245 nm. The 245 nm wavelength was chosen for the normalization point because the negative CD band in this region is not very sensitive to nucleotide conformation (11). While this procedure leads to agreement between calculation and "normalized" experiment for the negative band, the positive band, which is rather sensitive to the conformation (11,12), still may show substantial disagreement. Table 2 lists both the normalization factors and the standard deviations obtained when the normalized experimental data is compared with the calculated spectra. The larger normalization factors for the 12- and 17-bp DNAs may be attributed to an increased error in extrapolating for these short helices.

DISCUSSION

This study is the first attempt to compare the experimentally determined CD spectra of short, sequenced, homogeneous DNA fragments with calculated spectra. The calculated matrices are based on the assumption that

TABLE 2. Agreement between experiment and calculation for different T-matrices[a].

No. of base pairs in the fragments[b]	σ_{14}	Normalization factor[c] to T-matrix 14	σ_{14} normalized[d]	σ_1	Normalization factor[c] to T-matrix 1	σ_1 normalized[d]	σ average of calc. spectra[e]
12	0.80	1.29	0.60	0.52	1.17	0.45	0.64
17	0.52	1.27	0.22	0.75	1.38	0.85	0.51
22	0.49	0.99	0.50	0.47	0.98	0.47	0.31
27	0.44	1.14	0.38	0.67	1.16	0.73	0.52
43	0.51	0.98	0.51	0.54	1.12	0.63	0.27
64	0.20	1.00	0.20	0.56	1.08	0.65	0.29
69	0.31	0.96	0.32	0.36	1.04	0.39	0.19
76	0.51	0.99	0.51	0.39	1.05	0.44	0.18
84	0.39	1.08	0.37	0.44	1.07	0.49	0.23
95	0.28	1.07	0.28	0.47	1.18	0.62	0.21
258	0.34	0.98	0.35	0.43	1.02	0.44	0.18
360	0.50	1.22	0.44	0.63	1.39	0.78	0.37

a) Standard deviation values were calculated as described in the text. Subscripts to the letter sigma indicate the T-matrix used for the calculated curve.
b) As in Table 1, single stranded ends are not counted.
c) Normalization factor = $\Delta\varepsilon_{245}$ calculated/$\Delta\varepsilon_{245}$ measured.
d) These columns compare the normalized experimental data to the calculated spectra.
e) The average of calculated spectra is described in the text.

nearest neighbor contributions dominate the CD of a DNA double helix (16). Our goals were to examine the validity of this assumption and to further evaluate the dependence of local DNA structure on the nucleotide sequence.

Two different T-matrices were used in producing the calculated spectra. T-matrix 14 was chosen because previously it produced the best overall agreement with the experimental data (15). T-matrix 1 was used here because it incorporated data from the homopolymers $d(G)_n \cdot d(C)_n$ and $d(A)_n \cdot d(T)_n$. The greatly altered spectra (8) produced by these homopolymers, as opposed to polynucleotides with repeating sequences, is the cause of the dramatically different calculated spectra that result from the use of one matrix as opposed to the other (Figs. 2-4).

Compensating differences are observed in the spectra produced with the two T-matrices. T-matrix 14 generally predicts a positive band of greater amplitude than the measured band and shifted slightly to the longer wavelength. T-matrix 1, on the other hand, generally predicts a positive band of lesser amplitude than the measured band and slightly shifted to the shorter wavelengths. This observation led to the comparison of the measured spectra to an average of the two calculated spectra. It is interesting that the average of the spectra from T-matrix 1 and T-matrix 14 comes closer to the observed spectra than either of the calculations individually (Table 2). Thus, the contributions from AA, TT, GG, and CC are underestimated in T-matrix 14, but full inclusion of the homopolymer spectra is not warranted either. It is clear that the measured spectra correlate to the polymer data in a more complicated way than allowed for in either basis set considered individually in the nearest neighbor algorithm. Supporting this conclusion, the expected dependence of standard deviation on the length of the DNA fragment is not readily observed when either the normalized or unnormalized sigma values from the comparison of T-matrix 14 calculated spectra and the experimental data are plotted as a function of fragment length (Fig. 5). The same lack of correlation is also observed when the sigma values comparing T-matrix 1 curves with the experimental data are plotted (data not shown). However, when the standard deviation of the measured spectra and the average of the calculated spectra is plotted versus length of the DNA fragment, a much clearer length dependence is observed. Fig. 5 shows this length dependence and suggests that DNA fragments smaller than the 43-bp DNA may exhibit larger deviations because end effects are not considered in the nearest neighbor hypothesis.

Aside from the four smallest DNAs and the 360-bp fragment, the agree-

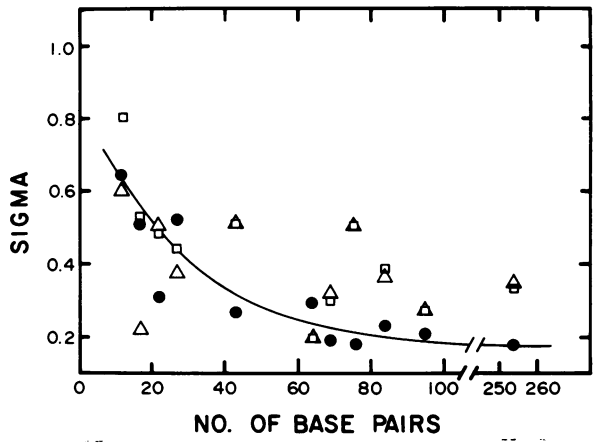

Figure 5. Dependence of standard deviation on fragment length. The standard deviation between the average of the two calculated spectra and the measured spectra is plotted as a function of fragment length (●). The normalized (△) and unnormalized (□) sigma values from the comparison of the T-matrix 14 calculated curves are also shown for comparison.

ment between measurement and calculation is good for the negative CD band at approximately 245 nm. This observation is not very surprising because this CD band is generally interpreted to be the result of base stacking rather than special conformational features of the double helix (11). The positive CD band at approximately 270 nm, however, does not agree nearly as well as the negative band. This is very interesting because that part of the CD spectrum has been shown to be especially sensitive to conformation (4,11,41).

A number of different approaches were employed in attempts to rationalize the deviations observed between the measured and calculated spectra on the basis of the known sequences. It was expected, for example, that molecules having a higher percentage of AA, TT, CC, and GG, would show increased agreement in their spectra to the spectra calculated with T-matrix 1. When spectral deviations were compared to the percentage of AA, TT, CC, and GG present in the DNAs however, no clear relationship was observed. In addition, no significant relationship of spectral deviation with either % AT or overall strand bias was found (data not shown).

In the case of the 17-, 27-, and 95-bp fragments, a relatively good agreement of observed and calculated spectra is obtained with T-matrix 14. When these spectra are compared with T-matrix 1 calculated spectra, however,

the standard deviation (Table 2) is greatly increased. To a lesser extent, this situation is reversed in the case of the 76-bp fragment whose σ value is greater with T-matrix 14 than T-matrix 1. These observations led to a consideration of whether next nearest neighbors might significantly influence the agreement. The nearest neighbor calculations explicitly recognize only dinucleotide pairs present in the basis set polymers. As well as these explicitly recognized nearest neighbors, however, each basis set and T-matrix carries with it an implicit set of next nearest neighbors depending on the polymer set chosen. Thus, it might be anticipated that spectral deviations would correlate with the fraction of next nearest neighbor bases present in the DNAs that are also present in the basis sets and resulting T-matrices.

Fig. 6 shows that some correlation is observed for the 27-, 43-, 76-, and 95-bp fragments between the standard deviation of the measured and calculated spectra and the fraction of next nearest neighbors included in the T-matrices. The 84-bp fragment is better fit by both T-matrices than expected on the basis of the included fraction of next nearest neighbors. As expected, the 360-bp fragment is not predicted well by either T-matrix (42, 43) due to its high AT-content (70.6%). The explicit inclusion of next

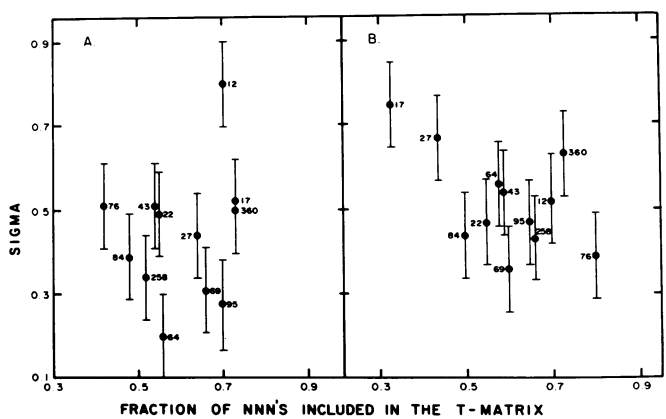

Figure 6. Correlation of standard deviation with fraction of included next nearest neighbors. Panels A and B illustrate the relationship between the unnormalized standard deviations for T-matrix 14 (A) and T-matrix 1 (B) and the fraction of next nearest neighbors present in both the DNA sequences of the fragments and the basis sets of the respective T-matrices. The numbers in both panels refer to the size of the DNA fragments in bps. The error bars (±0.10) are indicative of the overall reproducibility in the shape of the experimental curves.

nearest neighbors may partially account for some of the observed spectral deviations. The 69- and 84-bp fragments are much better fit by T-matrix 1 than expected on the basis of the fraction of next nearest neighbors. The same is true for the 64-bp fragment with respect to the spectra produced by T-matrix 14. These results strongly suggest that interactions extending to next nearest neighbors and perhaps longer range interactions are reflected in the shape of the positive band of the CD spectrum for a given polynucleotide.

A number of difficulties occur in the attempt to use the nearest neighbor approximation for the interpretation of the experimentally measured data. These difficulties are caused by at least two interlocking assumptions in the approximation. First, it is assumed that the interactions of a single base with any other bases more than one removed along the polymer chain are negligible. Second, it is assumed that the optically active conformation of the dinucleotide in the sequence being analyzed is the same as that present in the synthetic repeating polynucleotide from which the particular spectral component is derived.

With regard to the first assumption, in principle it is possible to construct a T-matrix which explicitly takes into account next nearest neighbors. At present, however, this cannot be done because there is not enough polymer data available. While our results (Fig. 6) suggest that the future use of a next nearest neighbor matrix would improve the agreement, this logical extension of the technique does not address the second related assumption of sequence specific conformations. This second assumption suggests that the individual dinucleotides considered along the entire helix contribute evenly to the overall conformation and in the same way as when they are present in a synthetic repeating polymer. The results obtained in the present study argue against this extrapolation from the polymer data and suggest that specific conformations, present in the polymers, are damped or averaged out to a greater degree than predicted by the nearest neighbor approximation.

ACKNOWLEDGEMENTS

This work was supported by grants from the N.I.H. (CA-20279) and the N.S.F. (PCM 15033). W.H. was supported, in part, by the Max Kade Foundation and the Deutsche Forschungsgemeinschaft. We thank W.W. Cleland for the use of the Jasco spectropolarimeter and D.M. Gray for communicating unpublished polymer CD data.

*Present address: Institut für Organische Chemie und Biochemie, Technische Hochschule Darmstadt, Petersenstraße 22, D-6100 Darmstadt, FRG.

REFERENCES

1. Cantor, C.R. and Schimmel, P.L. (1980) Biophysical Chemistry, III, Freeman and Company, San Francisco, CA.
2. Wells, R.D., Goodman, T.C., Hillen, W., Horn, G.T., Klein, R.D., Larson, J.E., Müller, U.R., Neuendorf, S.K., Panayotatos, N., and Stirdivant, S.M. (1980) Progress in Nucleic Acid Research and Molecular Biology 24, 167-267.
3. Tunis-Schneider, M.J.B. and Maestre, M.F. (1970) J. Mol. Biol. 52, 521-541.
4. Ivanov, V.I., Minchenkova, L.E., Schyolkina, A.K., and Poletayev, A.I. (1973) Biopolymers 12, 89-110.
5. Pohl, F.M. and Jovin, T.M. (1972) J. Mol. Biol. 67, 375-396.
6. Klysik, J., Stirdivant, S.M., Larson, J.E., Hart, P.A. and Wells, R.D. (1981) Nature, in the press.
7. Gray, D.M. and Ratliff, R.L. (1975) Biopolymers 14, 487-498.
8. Wells, R.D., Larson, J.E., Grant, R.C., Shortle, B.E., and Cantor, C.R. (1970) J. Mol. Biol. 54, 465-497.
9. Allen, F.S., Gray, D.M., Roberts, G.P., and Tinoco, I., Jr. (1972) Biopolymers 11, 853-879.
10. Gray, D.M., Morgan, A.R., and Ratliff, R.L. (1978) Nucleic Acids Res. 5, 3679-3695.
11. Sprecher, C.A., Baase, W.A., and Curtis-Johnson, W., Jr. (1979) Biopolymers 18, 1009-1019.
12. Zimmer, C. and Luck, G. (1974) Biochim. Biophys. Acta 361, 11-32.
13. Gray, D.M., Lee, C.S., and Skinner, D.M. (1978) Biopolymers 17, 107-114.
14. Hillen, W. and Wells, R.D. (1980) Nucleic Acids Research 8, 5427-5444.
15. Gray, D.M., Hamilton, F.D., and Vaughan, M.R. (1978) Biopolymers 17, 85-106.
16. Gray, D.M. and Tinoco, I., Jr. (1970) Biopolymers 9, 223-244.
17. Hillen, W., Klein, R.D., and Wells, R.D. (1981) Biochem., in press.
18. Hardies, S.C., Patient, R.K., Klein, R.D., Ho, F., Reznikoff, W.S., and Wells, R.D. (1979) J. Biol. Chem. 254, 5527-5534.
19. Hardies, S.C., and Wells, R.D. (1979) Gene 7, 1-14.
20. Panayotatos, N. and Wells, R.D. (1979) J. Biol. Chem. 254, 5555-5561.
21. Patient, R.K., Hardies, S.C., Larson, J.E., Inman, R.B., Maquat, L.E., and Wells, R.D. (1979) J. Biol. Chem. 254, 5548-5554.
22. Panayotatos, N. and Wells, R.D. (1979) J. Mol. Biol. 135, 91-109.
23. Panayotatos, N. and Wells, R.D. (1979) Nature 280, 35-39.
24. Patient, R.K. (1979) Nucleic Acids Res. 6, 2647-2665.
25. Horn, G.T. and Wells, R.D. (1981) J. Biol. Chem. 256, 2003-2009.
26. Early, T.A., Kearns, D.R., Hillen, W. and Wells, R.D. (1980) Nucleic Acids Res. 8, 5795-5812.
27. Early, T.A., Kearns, D.R., Hillen, W. and Wells, R.D. (1981) Biochem., in the press.
28. Early, T.A., Kearns, D.R., Hillen, W. and Wells, R.D. (1981) Biochem., in the press.
29. Wells, R.D., Hardies, S.C., Horn, G.T., Klein, B., Larson, J.E., Neuendorf, S.K., Panayotatos, N., Patient, R.K. and Selsing, E. (1980) Methods in Enzymology 65, 327-347.
30. Hardies, S.C., Hillen, W., Goodman, T.C. and Wells, R.D. (1979) J. Biol. Chem. 254, 10128-10134.

31. Hillen, W., Goodman, T.C. and Wells, R.D. (1981) Nucleic Acids Res. 9, 415-436.
32. Hillen, W., Goodman, T.C., Benight, A.S., Wartell, R.M. and Wells, R.D. (1981) J. Biol. Chem. 256, 2761-2766.
33. Horn, G.T. and Wells, R.D. (1981) J. Biol. Chem. 256, 1998-2002.
34. Wartell, R.M., Klysik, J., and Wells, R.D., unpublished results.
35. Gray, D.M., personal communication.
36. Hershfield, V., Boyer, H.W., Chow, L., and Helinski, D.R. (1976) J. Bacteriol. 126, 447-453.
37. Ohmori, H. and Tomizawa, J. (1979) Molec. Gen. Genet. 176, 161-170.
38. Tomizawa, J., personal communication.
39. Maxam, A.M. and Gilbert, W. (1977) Proc. Natl. Acad. Sci., U.S.A. 74, 560-564.
40. Oka, A., Nomura, N., Morita, M., Sugisaki, H., Sugimoto, K., and Takanami, M. (1979) Molec. Gen. Genet. 172, 151-159.
41. Chan, A., Kilkuskie, R., and Hanlon, S. (1979) Biochem. 18, 84-91.
42. Helleiner, C.W. and Verpoorte, J.A. (1974) Can. J. Biochem. 52, 582-585.
43. Cech, C.L. and Tinoco, I., Jr. (1977) Biopolymers 16, 43-65.